Naphthalimide-based macrophage nucleus imaging probes

Francisco Fueyo-González, Mar Fernández-Gutiérrez, Diego García-Puentes, Angel Orte, Juan A. González-Vera, Rosario Herranz

PII: S0223-5234(20)30378-0

DOI: https://doi.org/10.1016/j.ejmech.2020.112407

Reference: EJMECH 112407

To appear in: *European Journal of Medicinal Chemistry*

Received Date: 6 March 2020

Revised Date: 7 April 2020

Accepted Date: 27 April 2020

Please cite this article as: F. Fueyo-González, M. Fernández-Gutiérrez, D. García-Puentes, A. Orte, J.A. González-Vera, R. Herranz, Naphthalimide-based macrophage nucleus imaging probes, *European Journal of Medicinal Chemistry* (2020), doi: https://doi.org/10.1016/j.ejmech.2020.112407.

Naphthalimide-based macrophage nucleus imaging probes

Francisco Fueyo-González[a], Mar Fernández-Gutiérrez[c], Diego García-Puentes[d], Angel Orte[b], Juan A. González-Vera[a,b,*], Rosario Herranz[a,*]

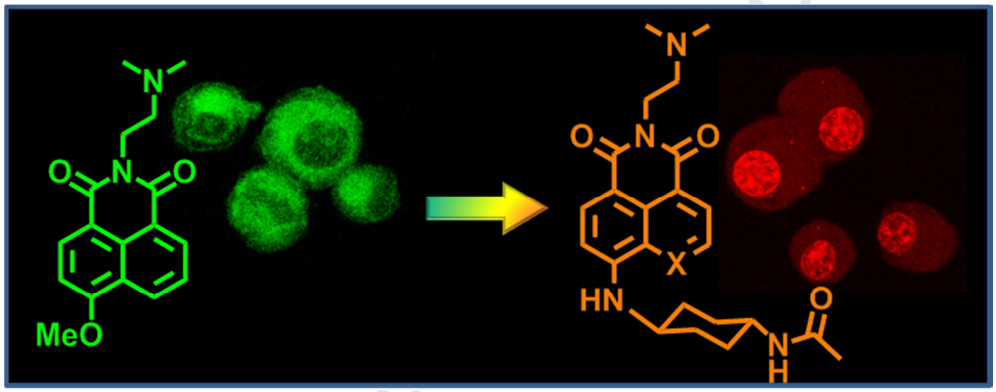

Naphthalimide-based macrophage nucleus imaging probes

Francisco Fueyo-González[a,e], Mar Fernández-Gutiérrez[b], Diego García-Puentes[c], Angel Orte[d], Juan A. González-Vera[a,d,*], Rosario Herranz[a,*]

[a]*Instituto de Química Médica (CSIC). Juan de la Cierva 3, 28006 Madrid, Spain.*

[b]*Instituto de Ciencia y Tecnología de Polímeros (CSIC), CIBER-BBN, Juan de la Cierva 3, 28006 Madrid, Spain.*

[c]*Instituto de Química Orgánica General (CSIC), Juan de la Cierva 3, 28006 Madrid, Spain.*

[d]*Departamento de Fisicoquímica, Unidad de Excelencia de Química Aplicada a Biomedicina y Medioambiente, Facultad de Farmacia, Universidad de Granada, Campus Cartuja, 18071, Granada, Spain.*

ABSTRACT

The photophysical properties of naphthalimide-based fluorophores can be easily tuned by chemical manipulation of the substituents on that privileged scaffold. Replacement of a OMe group at position 6 in 2-(hydroxyl)ethyl-naphthalimide derivatives by diverse amines, including 2-(hydroxyl)ethylamine, *trans*-(4-acetamido)cyclohexylamine and azetidine increases the solvatochromic (ICT) character, while this replacement in 2-(dimethylamino)ethyl-naphthalimide analogues (PET fluorophores) decrease their solvent polarity sensitivity or even reversed them to solvatochromic fluorophores. These fluorophores resulted macrophage nucleus imaging probes, which bind DNA as intercalants and showed low cytotoxicity in human cancer cells.

Keywords: Fluorescence probes; Naphthalimide derivatives; Quinolimide derivatives; Macrophage imaging probes; DNA intercalants

[*]Corresponding authors.

E-mail addresses: rosario@iqm.csic.es (R. Herranz); gonzalezvera@ugr.es (J. A. González-Vera)

[e] Current address: Department of Medicine, Translational Transplant Research Center, Immunology Institute, Icahn School of Medicine at Mount Sinai, New York, USA.

1. Introduction

Hydrophobicity or hydrophilicity of local environment determines interaction activities of proteins and controls the permeability of cell membrane compartments. Therefore, polarity-sensitive fluorophores are powerful chemical tools for studying biological systems. Donor-acceptor type dipolar fluorophores have been widely used in this field as intramolecular-charge-transfer (ICT) molecular probes [1-4]. Usually, these fluorophores exhibit red shifts in their emission spectra and a decrease in their fluorescence intensities upon increasing the environment polarity ("on-off" fluorophores). In spite of the numerous applications of ICT fluorophores in chemistry, biology and medical sciences, their low emission in aqueous media has limited their application for monitoring biological processes. On the other hand, the scarcity of polarity sensing fluorophores of type "off-on" when increasing the environment polarity, which include acridine [5], pyrene-3-carboxaldehyde [6], and 7-methoxy-4-methylcoumarin [7], has also limited the monitoring of biological processes that imply an increase in local hydrophilicity. Among the limited examples of this type of sensors, recently, 2-(*trans*-(4-hydroxy)-cyclohexylamino)-naphthalimide derivatives have been described as biothiol sensors [8], 2-(2-aminoethyl)-naphthalimide as *in cellulo* metal sensor [9], and some BODIPY derivatives as sensors of local hydrophilicity in dysfunctional lysosomes [10]. S. Singha et al. increased the emission intensity of diverse ICT fluorophores in water by replacing their dimethylamino group, usual donor group, by several dialkylamines or bulky monoalkylamines, preferably 2-(hydroxyl)ethylamine or *trans*-(4-acetamido)cyclohexyl-amine [8]. The increase of fluorescence was explained due to decreased non-radiative deactivation in H_2O, by hindering the interaction of the donor group with H_2O through hydrogen bonds. The increase in steric volume of the amino group also reduced its rotational freedom, facilitating the charge transfer.

We have recently described the switching from naphthalimide and quinolimide-based (ICT) fluorophores **1** (Figure 1) to PET fluorophores by the simple substituent manipulation of a hydroxyl to an *N*-dimethylamino group in analogues **2** [11]. This switch transformed the "on-off" polarity sensors *N*-(2-hydroxyethyl)-substituted derivatives **1a** and **1b** into the "off-on" polarity sensors *N*-(2-(dimethyl)aminoethyl)-substituted analogues **2a** and **2b**. In this way, we obtained H_2O and pH sensors and macrophage cytoplasm imaging probes. Now, with the aim of increasing the fluorescence emission of these fluorophores in H_2O, we have studied the replacement of the donor group OMe group of **1a**,**b** and **2a**,**b** by better donor groups, such as several substituted amines, concretely, 2-(hydroxy)ethylamine (Figure 1, **3** and **6**), *trans*-(4-acetamido)cyclohexylamine (Figure 1, **4** and **7**) and the good electrodonor group azetidine [12] (Figure 1, **5** and **8**). In general, this substituent manipulation has led to significant enhancements in the quantum yields of these fluorophores in water. We have also explored their application as *in cellulo* imaging probes in macrophages, multi-functional immune cells with key roles in host defense and tissue remodeling, which have been widely used as models for imaging cellular activity [13-15]. We have found a striking capability of most of the dyes to cross the nuclear membrane and bind DNA, acting as efficient macrophage nuclei staining probes.

Fig. 1. New Naphthalimide- and quinolimide-based fluorophores **3-8**

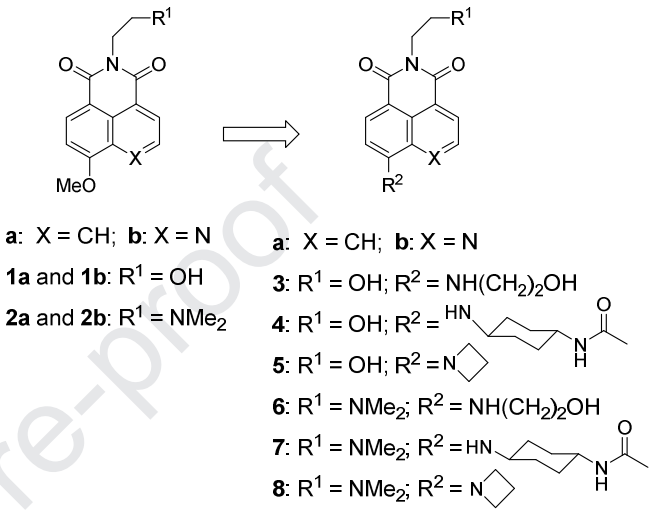

2. Results and discussion

2.1. Synthesis

As shown in Scheme 1, the 6-amino-naphthalimide derivatives **3a, 5a, 6a** and **8a** were obtained from the corresponding 6-bromo-naphthalimides **9a** and **10a** via aromatic nucleophile substitution, by treatment with the corresponding amine in EtOH at 120 ºC under MW irradiation. In the case of the substitution with *trans*-4-amino-cyclohexylamine in naphthalimides **11a** and **12a**, it was necessary to carry out the reaction in sealed tube at 150-180ºC in the presence of diisopropylethylamine (DIPEA). The acetylation of the free amino group of **11a** and **12a**, by treatment with acetic anhydride in CH_2Cl_2 yielded the naphthalimides objective **4a** and **7a**. A similar methodology was applied for the synthesis of the 9-[*trans*-(4-acetamido)cyclohexylamino-quinolimide **7b** from the corresponding 9-methoxy-quinolimide **2b**.

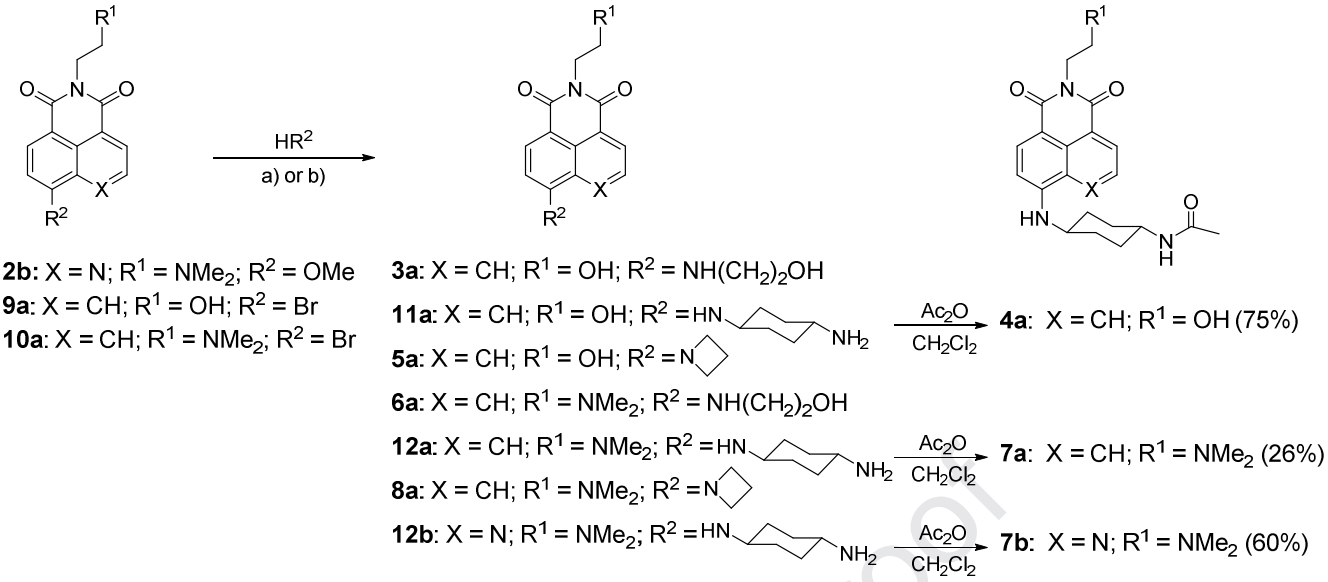

Scheme 1. Synthesis of the naphtalimide derivatives **3a-8a** and the quinolimide analogue **7b** (a) 2-Hydroxyethylamina or azetidine, EtOH, MW 120ºC (20-85%); (b) *trans*-(4-amino)cyclohexylamine, DIPEA, EtOH, 150-180ºC (2-91%).

2.2. Photophysical properties

We performed a thorough photophysical study of the properties of the new naphthalimides **3a**-**8a** and the quinolimide **7b** in solvents of diverse polarity (Table 1), in order to rationalize the effect of new R^2 substituents, when compared with the OMe-substituted compounds **1a** and **2a** (naphthalimides) and **2b** (quinolimide) in comparison with those of **1a**, **2a** and **2b**, respectively.

The replacement of the OMe group in the naphthalimide carrying the 2-(hydroxyl)ethyl chain at position 2, **1a**, by amines led to increases in the solvatochromic behavior characteristic of ICT–based fluorophores in **3a**-**5a**. These naphthalimides showed 65-100 nm bathochromic shifts in λ_{max}^{abs} and λ_{max}^{em} with respect to **1a**. The increase in the solvent polarity produced 10-40 nm bathochromic shifts in both wavelength maxima, increased the extinction coefficients and decreased the quantum yields.

In the naphthalimide carrying the 2-(dimethylamino)ethyl chain, **2a,** and in the quinolimide analogue, **2b**, the replacement of the OMe group by amines (compounds **6a**-**8a** and **7b**) also produced bathochromic shifts of 65-100 nm in λ_{max}^{abs} and λ_{max}^{em}. Also, these wavelengths increased with solvent polarity, except for the quinolimide derivative **7b**, where λ_{max}^{em} augmented from CH_3Cl to acetone and decreased from this solvent to H_2O. This behavior could be due to emission from two different excited states, the local excited (LE) and the ICT state [16, 17]. In the less polar solvents (CH_3Cl, dioxane and acetone) **7b** would emit from the ICT state (higher λ_{max}^{em}), while in more polar solvents (F_3C-CH_2OH, MeOH and H_2O) it would emit from the higher energy LE state. The effect of the replacement of the OMe group upon ε and Φ_F of the naphthalimide derivatives **6a**-**8a** and the quinolimide **7b** was diverse. In the azetidine derivative **8a** and the quinolimide **7b**, the PET effect that we had observed in **2a** and **2b** was absent, showing a solvatochromic behavior (typical of ICT fluorophores). In the naphthalimides **6a** and **7a** the ε coefficients decreased, while Φ_F increased, mainly in non-polar solvents, eliminating the off-on polarity effect previously observed in **2a**. Therefore, in the solvatochromic fluorophore **1a**, the replacement of the MeO group by hydroxyethylamine, azetidine or *trans*-(4-acetamido)cyclohexylamine enhanced the solvatochromic (ICT) character, while in the PET fluorophores **2a,b**, that replacement hinder the PET effect, leading either to solvatochromic fluorophores in the case of the azetidine derivative **8a** and the quinolimide **7b** or to low solvent polarity sensitivity in the (hydroxyethyl)amine (**6a**) or the *trans*-(4-acetamido)cyclohexylamine (**7a**) derivatives.

Table 1. Photophysical properties of the naphthalimides **1a**-**8a** and the quinolimides **2b** and **7b**.

Compd[a]	Solvent	λ_{max}^{abs} (nm)	ε ($M^{-1}cm^{-1}$)	λ_{max}^{em} (nm)	Φ_F [b]
1a	$CHCl_3$	360	14540	428	0.57
	Dioxane	359	12080	426	0.60
	Acetone	357	13610	434	0.43
	F_3C-CH_2OH	373	11950	449	0.32
	MeOH	366	12790	442	0.57
	H_2O	375	9650	458	0.30
2a	$CHCl_3$	366	8100	428	0.20
	Dioxane	358	6700	425	0.22
	Acetone	359	9700	433	0.14
	F_3C-CH_2OH	371	10100	450	0.63
	MeOH	367	8300	444	0.50
	H_2O	376	7200	460	0.63
3a	$CHCl_3$	428	11730	502	0.86
	Dioxane	422	11370	501	0.97
	Acetone	430	11570	516	0.82
	F_3C-CH_2OH	438	9970	523	0.55
	MeOH	438	12790	525	0.26
	H_2O	445	15780	527	0.17
4a	$CHCl_3$	433	10170	497	0.98
	Dioxane	426	13120	491	0.84
	Acetone	435	8400	510	0.77
	F_3C-CH_2OH	450	9230	524	0.51
	MeOH	447	8860	522	0.56
	H_2O	451	10630	527	0.23
5a	$CHCl_3$	443	13620	510	0.98
	Dioxane	428	10820	501	0.68
	Acetone	437	11380	521	0.72
	F_3C-CH_2OH	449	12720	527	0.44
	MeOH	449	14580	528	0.40
	H_2O	460	18660	533	0.16
6a	$CHCl_3$	426	6570	501	0.61
	Dioxane	422	5810	499	0.69
	Acetone	433	6190	511	0.99
	F_3C-CH_2OH	437	7530	530	0.56
	MeOH	438	4360	527	0.94
	H_2O	445	5220	531	0.57
7a	$CHCl_3$	430	6900	499	0.51
	Dioxane	422	3600	489	0.35
	Acetone	436	6700	511	0.77
	F_3C-CH_2OH	452	8300	529	0.40
	MeOH	441	7320	525	0.66
	H_2O	446	8170	534	0.71
8a	$CHCl_3$	441	9800	506	0.81
	Dioxane	430	10380	502	0.78
	Acetone	437	8510	518	0.87
	F_3C-CH_2OH	453	11830	534	0.20
	MeOH	449	7320	527	0.32
	H_2O[c]	460	6540	533	0.18
2b	$CHCl_3$	377	3100	457	0.12
	Dioxane	367	2800	457	0.17
	Acetone	370	4900	467	0.04
	F_3C-CH_2OH	380	2900	495	0.63
	MeOH	376	3700	493	0.23
	H_2O	381	3200	505	0.26
7b	$CHCl_3$	470	3900	554	0.16
	Dioxane	466	3470	562	0.12
	Acetone	462	4020	572	0.03
	F_3C-CH_2OH	483	4225	539	0.02
	MeOH	471	3040	526	0.05
	H_2O	471	3800	533	0.02

[a]Measured in duplicate at a 12 μM concentration. [b]Quantum yields calculated with reference to cumarine 153 (in EtOH), except for **1a**, **2a** and **2b**, where the reference was quinine sulfate (in 0.1 M H_2SO_4).

2.3. Cytotoxicity in tumor cells

Several 2-[2-(dimethylamino)ethyl]-naphthalimide derivatives have been described as antitumor agents [18], such as mitonafide or amonafide [19, 20], which bind to DNA as intercalants and inhibit topoisomerase II [21], forming and stabilizing the ternary complex DNA-intercalant-topoisomerase II [22]. Besides, some quinolimide derivatives have been also reported as antitumor compounds [23]. Taking into account these reports, the naphthalimide and quinolimide derivatives herein described were included in a high throughput screening (HTS) for cytotoxicity in non-small cell lung cancer (A549), colon (HT29), breast (MDA-MD231), and pancreas (PSN1) human cancer cell lines, using doxorubicin as positive control and according to the National Cancer Institute (NCI) protocols. None of the 2-(hydroxyl)ethyl-naphthalimide derivatives **3a**-**5a** showed citotoxicity at the highest tested concentration (40 μM). In the 2-(dimethylamino)-ethyl analogues, the naphthalimides **6a** and **7a** and the quinolimide **7b** showed low cytotoxicities in the μM range as the corresponding 6-methoxy-naphthalimide **2a** and the 9-methoxy-quinolimide derivative **2b** (Table 2). These values of cytotoxicity were of the same order than those previously reported for mitonafide and amonafide [18, 23].

Table 2. Cytotoxicities (GI_{50})[a] of 2-(2-(dimethylamino)ethyl-naphthalimides and 5-(2-(dimethylamino)ethyl-quinolimides

Compd	Lung A549	Colon HT29	Breast MDA-MD-231	Pancreas PSN1	Mouse macrophages
Doxorubicin	0.085	0.109	0.055	0.052	ND[b]
2a	11.40	9.39	16.10	16.10	36.3
2b	>33.4	>33.4	>33.4	>33.4	ND[b]
6a	11.90	9.77	10.10	13.70	38.1
7a	7.55	3.79	5.44	8.05	33.3
8a	>30.9	>30.9	>30.9	>30.9	20.8
7b	7.79	5.67	8.26	9.44	5.8

[a]μM concentrations. [b]ND: Non determined

2.4. Macrophage imaging probes

As already commented, although there are diversity of fluorescent probes for imaging specific cellular organelles [24-31], the number of polarity sensing fluorophores with “off-on” features when increasing the environment polarity is very limited and, in general, they have demonstrated limited application due to quenching of their fluorescence by protonation and to their low excitation and emission wavelengths [32]. The scarcity of this type of fluorophores, which emit in polar media, has limited the monitoring of biological processes that imply an increase in local

hydrophilicity. In view of the photophysical behavior and low cytotoxicity of the naphthalimides and quinolimides herein described, we explored their application as *in cellulo* imaging probes in macrophages. Therefore, mouse macrophages were treated with a 5 μM concentration of each fluorophore and, after one hour of incubation at 37 °C, the cells were visualized by confocal microscopy. After laser excitation at 488 nm, the emission of the new naphthalimides **3a**-**8a** was observed with a 505-570 nm filter, while the emission of the quinolimide **7b** was observed with the GFP filter (525-615 nm). We also compare these results with the images of previously published compounds **1a,b** and **2a,b**. As shown in Figures 2 and 3, cells treated with the fluorophores carrying the 2-(hydroxyl)ethyl chain at the imide ring **1a,b** and **3a**-**5a** (Figure 2, A, C, and E, G, I) showed lower fluorescence than cells treated with fluorophores carrying the 2-(dimethylamino)ethyl chain **2a,b**, **6a**-**8a** and **7b** (Figure 2, B, D, F, H, J and K), which displayed bright fluorescence. As already described, cells treated with the 6-methoxy-naphthalimide **2a** or the 9-methoxy-quinolimide **2b** displayed bright fluorescence at their cytoplasm (Figure 2, B and D), while cells treated with the 6-substituted amino-naphthalimides **3a**-**8a** or the quinolimide **7b** displayed the fluorescence at their nucleus (Figure 2, F, H, J, K), except for the cells treated with the azetidine derivative **5a**, which displayed low fluorescence at the cytoplasm (G). According to the Φ_F of these fluorophores in H_2O, cells treated with the *trans*-(4-acetamido)-cyclohexylamine derivative **7a** (Figure 2, F) showed much brighter fluorescence than the corresponding 2-(hydroxyl)ethyl analogue **6a** (Figure 2, J). Interestingly, cells treated with the naphthalimide derivative **8a** (Figure 2, H) or with the quinolimide **7b** (Figure 2, K) displayed bright fluorescence, in spite of the low Φ_F of these fluorophores in H_2O (78-86% lower than in $CHCl_3$ or dioxane). This would indicate their localization in a hydrophobic environment in the nucleus.

The nucleus is the most prominent organelle of cells, where ribosome synthesis and gene expression are regulated [33], so its visualization is important to help answer questions about these processes and others such as the genesis of tumors or the action of some drugs. Among the limited number of known nuclear fluorophores, 4',6-diamidino-2-phenilindole (DAPI) and the Hoechst dyes, which bind to the minor groove of DNA, and propidium iodide (PI), DNA intercalant, have been the most used probes to stain cell nuclei, due to its good cellular permeability and its specificity for DNA [34]. However, these fluorophores are generally mutagenic, have low water solubility and low photostability, which limits their application in studies that require long observation times. Other small fluorophores, used for the visualization of the nucleus, such as, for example, various styryl derivatives [35, 36], fluorescein [37], ruthenium (II) dyes [38] and hemicianin [39], are used at very low concentrations, due to problems of fluorescence quenching by aggregation. In addition, these dyes usually suffer from notable photobleaching after photoexcitation [40]. Therefore, obtaining new nuclear probes, soluble in water, photostable and with low cytotoxicity is an objective of great interest for the visualization of the cell nucleus in long-term studies.

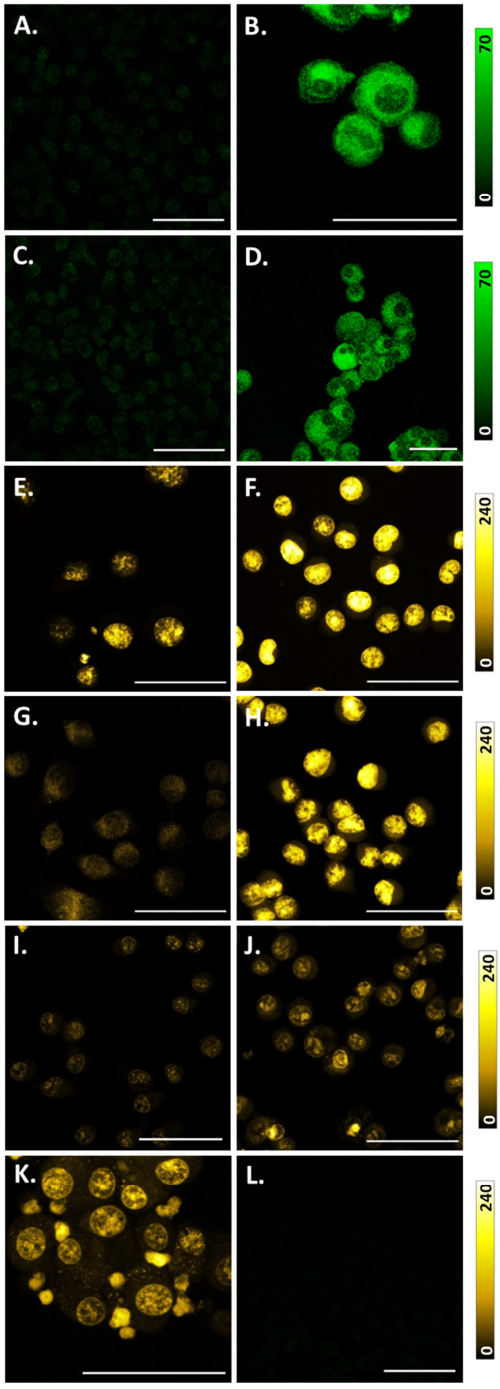

Fig. 2. Confocal microscopy images of mouse macrophages treated with a 5 μM concentration of A) naphthalimide **1a**; B) naphthalimide **2a**; C) quinolimide **1b**; D) quinolimide **2b**; E) naphthalimide **4a**; F) naphthalimide **7a**; G) naphthalimide **5a**; H) naphthalimide **8a**; I) naphthalimide **3a**; J) naphthalimide **6a**; and K) quinolimide **7b**. L) Untreated control cells. Scale bars represent 50 μm.

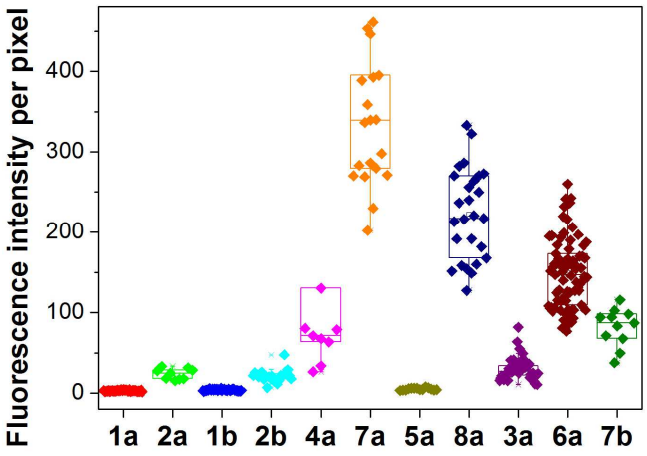

Fig.3. Fluorescence relative intensity of the probes in macrophages. Box-and-whisker plot represents the average fluorescence intensity in pixels of confocal images (in Fig. 2) containing the studied fluorophores in mouse macrophages treated with a 5 μM concentration of probe. Boxes correspond to the 25 and 75%, with a horizontal bar indicating the average value. Whiskers represent the minimum and maximum values.

Taking into account the clear nuclear localization of the naphthalimides carrying the 2-(dimethylamino)ethyl chain **6a**-**8a**, and the quinolimide **7b**, in order to help to elucidate their binding site, we explored whether these fluorophores co-localized with DAPI. As shown in Figure 4 for **7a**, the images obtained with our fluorophores overlapped completely with those obtained with DAPI, indicating coincidence in DNA binding (Pearson colocalization coefficient of 0.929 ± 0.06, Figure S5). In addition, two competition experiments were performed between **7a** and DAPI. In the first, a 1 μM concentration of DAPI was added to the macrophages and, after 1 hour of incubation at 37 °C and after checking that DAPI was in the nucleus, the naphthalimide **7a** was added in increasing concentrations from 1 to 10 μM. In the second experiment the order of addition of the fluorophores was changed, adding compound **7a** at 1 μM concentration and increasing concentrations of DAPI from 1 μM to 10 μM. In all cases, both fluorophores co-localized in the nucleus, without observing displacement between them. These results indicated that although both fluorophores bind to DNA, they do at concentrations far from saturation or binding to non-competing sites.

Taking into account the moderate cytotoxicity shown by **6a**-**8a** and **7b** in tumor cells, the cytotoxicity in mouse macrophages RAW 264.7 (ECACC, Sigma P11) was also determined by an Alamar blue assay [41]. After 24 h of incubation at 37 °C, increasing concentrations up to 100 μM of the studied fluorophores were added. All the compounds showed low cytotoxicity (Table 2), with GI_{50} values greater than 10 μM, except for the quinolimide **7b**, with a GI_{50} of 5.8 μM.

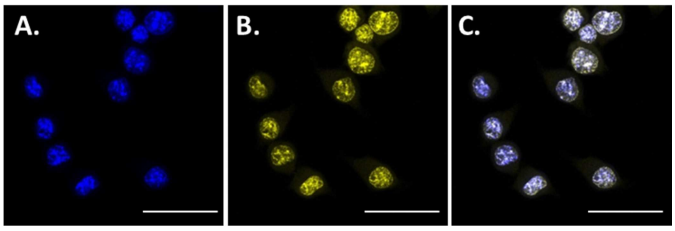

Fig. 4. Cellular co-localization of the nuclear dye DAPI and the 2-(2-(dimethylamino)ethyl)-naphthalimide derivative **7a** in macrophages at a 5 μM concentration. A) Macrophage cell nuclei stained with DAPI. B) Macrophage cell nuclei stained with naphthalimide **7a**. C) Overlay of the two channels. Scale bars represent 50 μm.

2.5. Binding to DNA

Having confirmed the nuclear localization of some of our fluorophores, we studied the interaction of the naphthalimide derivative **7a** and the quinolimide analogue **7b** with DNA, *in vitro*, using salmon sperm DNA (FS-DNA) and the double strand of the oligonucleotide R-13 (5'-GCGTACGCCAGCG-3') [42] as models of DNA. For this study, circular dichroism, UV spectrometry and fluorescence excitation spectra of the titration of constant concentrations of the fluorophores (**7a**: 16 μM and **7b**: 20 μM) with increasing concentrations of FS-DNA (8.1 μM till 2.0 mM base pairs) and oligonucleotide R-13 (0.165 μM till 4.4 mM) and the titration of a 4.3 μM concentration of this oligonucleotide with increasing concentrations of the fluorophores (0-430 μM) were recorded [43, 44]. The behavior of both **7a** and **7b** was similar. Their CD spectra showed a very small negative band at their respective absorption maxima wavelengths (**7a** ≈ 450 nm and **7b** ≈ 470 nm), indicative of their binding as intercalants. If the binding would have been to the major or minor DNA grooves, that band should have been stronger. Besides, the CD signal increases slightly by increasing the concentration of the fluorophore (shown in Figure 5 for **7a**). These results are characteristic of DNA intercalants [45]. Significant changes were also observed in the UV and fluorescence excitation spectra. The absorption intensity decreased, while fluorescence intensity increased with increasing DNA concentration. These results were also indicative of a binding as intercalant [46]. In the case of the quinolimide derivative **7b**, it was not possible to detect its fluorescence excitation, probably due to its low Φ_F in H_2O. These results would explain why although our fluorophores co-localizes with DAPI, there is no competition between them, since, as mentioned, DAPI binds to the minor DNA groove and is not intercalant.

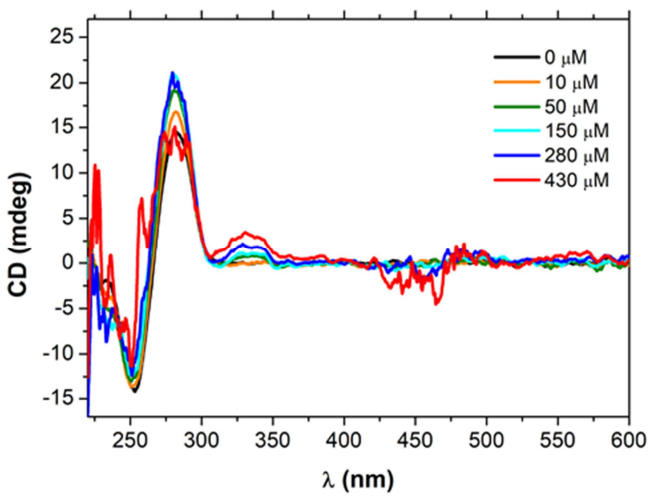

Fig. 5. CD spectra of R-13 with increasing concentrations of the naphthalimide **7a**.

Binding isotherms were obtained for **7a** and **7b** from the representation of the absorbance against the DNA concentration (Figures 6A and B). The affinity constants, expressed as dissociation constants K_d with the DNA concentration referred in terms of base pairs, were calculated from these isotherms (see Supplementary materials for details on the fittings), showing a good correlation between the results of FS-DNA and R-13. The K_d values of **7a** were 1.7 μM and 1.3 μM with FS-DNA and R-13, respectively, whereas K_d values of 8.9 μM and 3.5 μM were obtained for **7b** with FS-DNA and R-13, respectively. The stoichiometry of the interaction represents the number of sites (base pairs) occupied by the dyes upon binding. When interacting with FS-DNA, we obtained the binding of 1 molecule of **7a** for each 7 base pairs, and 1 molecule of **7b** for each 9 base pairs. The corresponding binding isotherms to the shorter oligonucleotide R-13 showed the binding of 1 molecule of **7a** for each 5 base pairs, and 1 molecule of **7b** for each 6 base pairs, indicating a higher level of saturation in the short strands

3. Conclusions

The results herein described show how the photophysical properties of naphthalimide-based fluorophores can be easily tuned by chemical manipulation of the substituents on that privileged scaffold. Thus, in the 2-(hydroxyl)ethyl-naphthalimides, replacement of the OMe group at position 6 by diverse amines leads to bathochromic shifts in their λ_{max}^{em} and to increases in their solvatochromic ICT character. However, in the PET fluorophores, 2-(dimethylamino)ethyl-naphthalimide derivatives, in general, that replacement leads to increases in the fluorescence quantum yields in all solvents, regardless of their polarity, loss of the PET character, and in some cases to highly solvatochromic fluorophores. Naphthalimides and quinolimides carrying the 2-(dimethylamino)ethyl chain at the imide ring have resulted good probes for macrophage imaging. While those with the MeO group at the aromatic ring localized at the cytoplasm, those where an amino moiety replaces the MeO group, such as **6a**-**7a** and **7b**, are localized at the nucleus, where they bind DNA as intercalants.

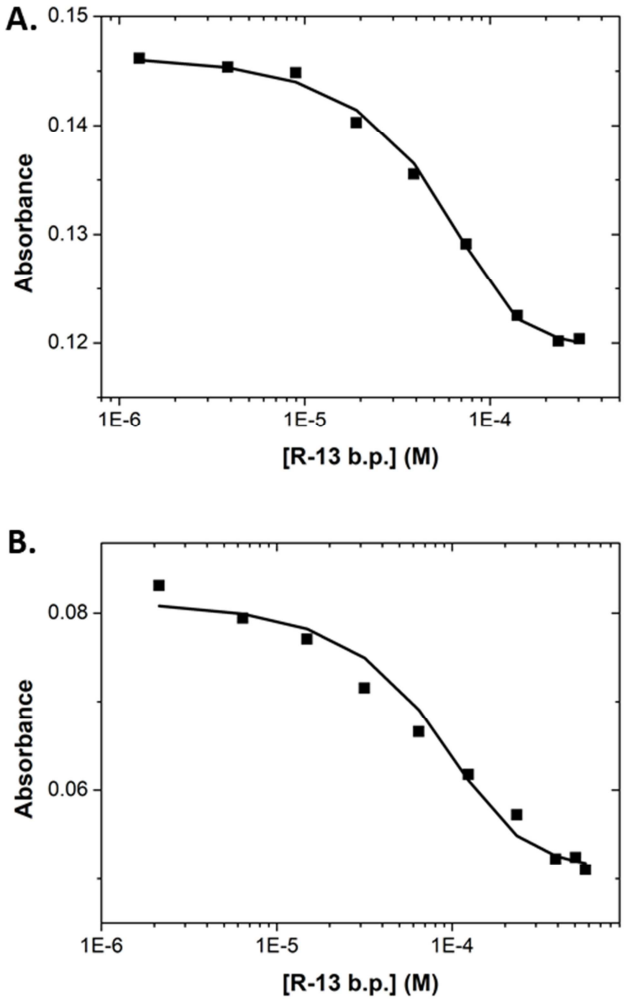

Fig. 6. Binding isotherms obtained for (A) **7a** and (B) **7b** from the representation of the absorbance against concentration of R-13.

4. Experimental

4.1. Synthesis

4.1.1. General methods

All reagents were of commercial quality. Solvents were dried and purified by standard methods. Analytical TLC was performed on aluminum sheets coated with a 0.2 mm layer of silica gel 60 F_{254}. Silica gel 60 (230-400 mesh) was used for flash chromatography. HPLC-MS was performed on a Sunfire C_{18} (4.6×50 mm, 3.5 μm) column at 30°C, with a flow rate of 1 mL/min and gradient of 0.1% of formic acid in CH_3CN (solvent

A) in 0.1% of formic acid in H_2O (solvent B) was used as mobile phase. Electrospray in positive mode was used for ionization. NMR spectra were recorded using Varian Inova or Mercury 400, and Varian Unity 500 spectrometers. The NMR spectra assignments were based on COSY, HSQC, and HMBC spectra. High resolution mass spectra (HRMS) were recorded on an Agilent 6520 Q-TOF instrument with an ESI source. MW experiments were carried out in sealed vessels in a MW Emrys™ Synthesizer (Biotage AB), with transversal IR sensor for reaction temperature monitoring. UV-visible spectroscopy measurements were made at 25 Cº on a Lambda 35, Perkin Elmer, UV-vis spectrophotometer; Starna Cells (16.100-Q-10) 100 µL sub-micro cuvette, 1 cm path length. Steady-state fluorescence emission spectra were performed at 25 Cº either on a PerkinElmer LS 50B luminescence spectrometer or a JASCO FP-8300 spectrofluorometer equipped with a 450 W xenon lamp for excitation; Starna Cells (16.100F-Q-10) 100 µL sub-micro cuvette, 1 cm path length.

*4.1.2. Synthesis of 6-bromo-2-(2-hydroxyethyl)-1*H*-benzo[*de*]isoquinoline-1,3(2*H*)-dione (**9a**)[47]*

2-Aminoethanol (48 µL, 0.79 mmol) was added to a solution of 6-bromo-1*H*,3*H*-benzo[*de*]isochromene-1,3-dione (200 mg, 0.72 mmol) in dry EtOH (3 mL) and the mixture was heated at 68 ºC under MW irradiation for 10 min. After cooling at room temperature, the precipitated solid was filtered and dried under vacuum for 12 h to yield the corresponding 6-bromo-naphthalimide **9a** as a yellow solid (205 mg, 90 %). M.p. 205 ºC. HPLC-MS (15-95 % gradient of A in B, 10 min) t_R = 8.07 min.^{1}H-NMR ($CDCl_3$, 400 MHz) δ: 2.19 (br s, 1H,), 3.92 (m, 2H), 4.39 (t, *J* = 5 Hz, 2H), 7.79 (dd, 1H, *J* = 7.5 and 8.5 Hz), 7.99 (d, *J* = 8 Hz, 1H), 8.36 (d, *J* = 8 Hz, 1H), 8.53 (dd, *J* = 1 and 8.5 Hz, 1H), 8.60 (dd, *J* = 1 and 7.5 Hz, 1H).^{13}C-NMR (CD_3OD, 100 MHz) δ: 43.0, 61.9, 122.1, 123.0, 128.3, 129.2, 130.8, 130.9, 131.4, 131.7, 132.5, 133.8, 164.7. HRMS (ESI) *m/z*: Calc. for $C_{14}H_{11}BrNO_3$ ($[M+H]^+$): 319.9917, Found: 319.9955 (0.09 %). Calc. for $(M+H)^+(-H_2O)$: 303.9792, Found: 303.9777 (100%).

*4.1.3. Synthesis of 2,6-bis(2-hydroxyethyl)-1*H*-benzo[*de*]isoquinoline-1,3(2*H*)-dione (**3a**)*

2-Aminoethanol (275 µL, 4.6 mmol) was added to a solution of the 6-bromo-naphthalimide **9a** (150 mg, 0.46 mmol) in EtOH (5mL) and the mixture was heated at 120 ºC under MW irradiation for 1.5 h. Afterwards, the solvent was evaporated to dryness and the residue was purified by flash chromatography, using 0-3% gradient of MeOH in CH_2Cl_2 as eluent, to give the desired 2,6-bis(2-hydroxyethyl)-naphthalimide **3a** as an orange solid (50 mg, 36 %). M.p. 209 ºC. HPLC-MS (5-95% gradient of A in B, 10 min) t_R = 5.62 min. ^{1}H-NMR (DMSO-d_6, 400 MHz) δ: 3.51 (c, 2H, *J* = 6 Hz,), 3.58 (t, 2H, *J* = 7 Hz), 3.71 (t, 4H, *J* = 6 Hz), 4.10 (t, 2H, *J* = 7 Hz), 6.75 (d, 1H, *J* = 8.5 Hz), 7.63 (t, 1H, *J* = 8 Hz), 7.70 (br s, 1H), 8.20 (d, 1H, *J* = 8.5 Hz), 8.38 (d, 1H, *J* = 7 Hz), 8.66 (d, 1H, *J* = 8.5 Hz). ^{13}C-NMR (DMSO-d_6, 100 MHz) δ: 41.3, 45.6, 57.9, 58.8, 103.7, 107.6, 120.0, 121.8, 124.1, 128.5, 129.3, 130.5, 134.0, 150.7, 162.9, 163.8. HRMS (ESI) *m/z*: Calc. for $C_{16}H_{16}N_2O_4$ ($[M+H]^+$): 301.1182, Found: 301.1176.

*4.1.4. Synthesis of 6-((*trans*-4-aminocyclohexyl)amino)-2-(2-hydroxyethyl)-1*H*-benzo[*de*]-isoquinoline-1,3(2*H*)-dione (**11a**)*

trans-1,4-Diaminocyclohexane (195 mg, 1.71 mmol) and DIPEA (28 µL, 0.51 mmol) were added to a solution of the 6-bromo-naphthalimide **9a** (110 mg, 0.343 mmol) in EtOH (5 mL) and the mixture was heated at 120ºC in a closed tube for 5 days. After cooling at room temperature, the precipitated solid was filtered off and the filtrate was evaporated to dryness to give the desired naphthalimide **11a** as a brown solid (110 mg, 91 %). M.p. 280 ºC. HPLC-MS (gradient 5-95% of A en B, 10 min) t_R = 4.61 min. ^{1}H-NMR (DMSO-d_6, 400 MHz) δ: 1.25 and 1.49 (2m, 4H), 1.85 and 2.02 (2m, 4H), 2.62 (m, 1H), 3.57 (t, 2H, *J* = 6.5 Hz), 3.61 – 3.65 (m, 1H), 4.11 (t, 2H, *J* = 6.5 Hz), 6.82 (d, 1H, *J* = 9 Hz), 7.30 (d, 1H, *J* = 8 Hz), 7.64 (t, 1H, *J* = 7 and 8.5 Hz), 8.23 (d, 1H, *J* = 9 Hz), 8.41 (dd, 1H, *J* = 1 and 7 Hz), 8.76 (dd, 1H, *J* = 1 and 8.5 Hz). ^{13}C-NMR (DMSO-d_6, 100 MHz) δ: 30.5, 34.8, 41.4, 49.9, 51.2, 58.0, 104.1, 107.4, 120.1, 121.9, 124.0, 128.8, 129.6, 130.6, 134.2, 149.8, 163.0, 163.9. HRMS (ESI) m/z: Calc. for $C_{20}H_{23}N_3O_3$ ($[M+H]^+$): 354.1812, Found: 354.1811.

4.1.5. Synthesis of N-*(*trans*-4-((2-(2-hydroxyethyl)-1,3-dioxo-2,3-dihydro-1*H*-benzo[*de*]isoquinolin-6-yl)amino)-cyclohexyl)acetamide (**4a**)*

Acetic anhydride (1mL) was added to a solution of the naphthalimide **11a** (40 mg, 0.11 mmol) in CH_2Cl_2 (5 mL) and the solution was stirred at room temperature for 30 min. Then, the reaction mixture was evaporated to dryness and the residue was purified by flash chromatography, using 0-5% gradient of MeOH in CH_2Cl_2 as eluent, to give the desired acetylated derivative **4a** as an orange solid (32 mg, 75%). M.p. 116 ºC. HPLC-MS (gradient 5-95% of A in B, 10 min) t_R = 7.29 min. ^{1}H-NMR (DMSO-d_6, 400 MHz) δ: 1.38 (m, 2H), 1.51 (m, 2H), 1.92 (s, 3H), 2.06 (m, 2H), 3.55 and 3.65 (2m, 2H), 4.28 (s, 4H), 6.89 (d, 1H, *J* = 8.5 Hz), 7.39 (d, 1H, *J* = 7.5 Hz), 7.68 (dd, 1H, *J* = 8.5 Hz), 7.82 (d, 1H, *J* = 7.5 Hz), 8.26 (d, 1H, *J* = 8.5 Hz), 8.44 (d, 1H, *J* = 8.5 Hz), 8.79 (d, 1H, *J* = 8.5 Hz). ^{13}C-NMR (DMSO-d_6, 100 MHz,) δ: 22.8, 30.5 and 31.0, 45.6, 47.3, 50.9, 61.1, 104.4, 107.2, 120.1, 121.6, 124.1, 129.1, 129.7, 130.8, 134.4, 150.0, 163.0, 164.0, 168.3. HRMS (ESI) *m/z*: Calc. for $C_{22}H_{25}N_3O_4$ ($[M+H]^+$): 396.1917, Found: 396.1918.

*4.1.6. Synthesis of 6-(azetidin-1-yl)-2-(2-hydroxyethyl)-1*H*-benzo[*de*]isoquinoline-1,3(2*H*)-dione (**5a**)*

Azetidine (178 µL, 2.65 mmol) was added to a solution of the 6-bromo-naphthalimide **9a** (170 mg, 0.53 mmol) in EtOH (5mL) and the mixture was heated at 120 ºC under MW irradiation for 1.5 h. After cooling at room temperature, the precipitated solid was filtered, washed with EtOH (3×1mL),

and dried under vacuum for 12 h to yield the corresponding 6-azetidin-1-yl-naphthalimide **5a** as a red solid (50 mg, 36 %). M.p. 222 ºC. HPLC-MS (gradient 5-95% of A in B, 10 min) t_R = 7.09 min. ^{1}H-NMR (DMSO-d_6, 400 MHz) δ: 2.47 (m, 2H), 3.59 (m, 2H), 4.09 (t, 2H, *J* = 7 Hz), 4.43 (t, 4H, *J* = 7.5 Hz), 4.79 (br s, 1H), 6.34 (d, 1H, *J* = 8.5 Hz), 7.52 (t, 1H, *J* = 8 Hz), 8.11 (d, 1H, *J* = 8.5 Hz), 8.24 (d, 1H, *J* = 8 Hz), 8.33 (d, 1H, *J* = 7 Hz). ^{13}C-NMR (DMSO-d_6, 100 MHz) δ: 16.4, 41.4, 55.0, 57.9, 105.8, 108.2, 120.0, 121.6, 123.7, 129.8, 130.5, 132.6, 151.9, 162.8, 163.7. HRMS (ESI) *m/z*: Calc. for $C_{17}H_{16}N_2O_3$ ([M+H]$^+$): 297.1233, Found: 297.1222.

*4.1.7. Synthesis of 2-(2-(dimethylamino)ethyl)-6-((2-hydroxyethyl)amino)-1*H*-benzo[*de*]isoquinoline-1,3(2*H*)-dione (**6a**)*

Ethanolamine (52 µL, 0.86 mmol) was added to a solution of the 6-bromo-naphthalimide **10a** [48] (50 mg, 0.14 mmol) in EtOH (5 mL) and the mixture was heated at 120ºC under MW irradiation for 3 h. Afterwards, the solvent was evaporated to dryness and the residue was purified by reverse C_{18} flash chromatography, using 0-30 % CH_3CN in H_2O gradient as eluent, to give the desired naphthalimide **6a** as yellow syrup (11 mg, 20%). HPLC-MS (5-95% gradient of A in B, 10 min) t_R = 4.36 min. ^{1}H-NMR (MeOD, 500 MHz) δ: 2.87 (s, 6H), 3.59 (t, 1H, *J* = 6 Hz), 3.88 (t, 1H, *J* = 6 Hz), 4.47 (t, 1H, *J* = 6 Hz), 6.86 (d, 1H , *J* = 8.5 Hz), 7.67 (dd, 1H, *J* = 7.5 and 8.5 Hz), 8.40 (d, 1H, *J*=8.5 Hz), 8.55 (m, 2H). ^{13}C-NMR (MeOD, 125 MHz) δ: 36.9, 44.6, 46.7, 58.0, 60.8, 105.3, 115.7, 122.0, 123.3, 125.6, 127.3, 129.7, 132.5, 136.3, 153.1, 165.9, 166.6. HRMS (ESI) *m/z*: Calc. for $C_{18}H_{21}N_3O_3$ ([M+H]$^+$): 328.1655, Found: 328.1661.

*4.1.8. Synthesis of 6-((*trans*-4-aminocyclohexyl)amino)-2-(2-(dimethylamino)ethyl)-1*H*-benzo[*de*]-isoquinoline-1,3(2*H*)-dione (**12a**)*

trans-1,4-Diaminocyclohexane (80 mg, 1.90 mmol) and DIPEA (26 µL, 0.46 mmol) were added to a solution of the 6-bromo-naphthalimide **10a** [48] (110 mg, 0.31 mmol) in EtOH (5 mL) and the mixture was heated at 120ºC in a closed tube for 2 days. Afterwards, the solvent was evaporated to dryness and the residue was purified by reverse C_{18} flash chromatography, using 0-15 % CH_3CN in H_2O gradient as eluent, to give the desired naphthalimide **12a** as dark yellow solid (38 mg, 32%). M.p. 178 ºC HPLC-MS (30-95% gradient of A in B, 10 min) t_R = 4.5 min. ^{1}H-NMR [$(CD_3)_2CO$, 400 MHz] δ: 1.34, 1.52 and 2.15 (3m, 8H), 2.12 (s, 6H), 2.42 (t, 2H, *J* = 7 Hz), 3.26 (m, 1H), 3.66 (m, 1H), 4.09 (t, 2H, *J* = 7 Hz), 6.54 (d, 1H, *J* = 7.5 Hz), 6.82 (d, 1H, *J* = 8.5 Hz), 7.50 (t, 1H, *J* = 8 Hz), 8.23 (d, 1H, *J* = 8.5 Hz), 8.35 (d, 1H, *J* = 7.5 Hz), 8.47 (d, 1H, *J* = 8.5 Hz). ^{13}C-NMR ($(CD_3)_2CO$, 100 MHz) δ: 30.0, 31.4 and 31.7, 36.9, 44.6, 51.0, 56.5, 58.0, 103.8, 108.5, 120.1, 122.3, 123.6, 127.1, 129.6, 130.0, 133.6, 149.0, 162.7, 163.5. HRMS (ESI) *m/z*: Calc. for $C_{22}H_{28}O_2N_4$ ([M+Na]$^+$): 403.2104, Found: 403.2091.

4.1.9. Synthesis of N-*(*trans*-4-((2-(2-(dimethylamino)ethyl)-1,3-dioxo-2,3-dihydro-1*H*-benzo[*de*]isoquinolin-6-yl)amino)-cyclohexyl)acetamide (**7a**)*

Acetic anhydride (1mL) was added to a solution of the naphthalimide **12a** (14 mg, 0.028 mmol) in (9:1) CH_2Cl_2/dry acetone mixture (1 mL) and the solution was stirred at room temperature for 6 h. Then, the reaction mixture was evaporated to dryness and the residue was purified by flash chromatography, using 1-10% gradient of MeOH in CH_2Cl_2 as eluent, to give the desired acetylated derivative **7a** as an orange solid (12 mg, 80%). M.p. 241 ºC. HPLC-MS (30-95% gradient of A in B, 10 min) t_R = 1.87 min. ^{1}H-NMR (CD_3OD, 500 MHz) δ: 1.39 (m, 2H,), 1.51 (m, 2H), 1.85 (s, 3H), 1.94 (m, 2H), 2.11 (m, 2H), 2.76 (s, 6H), 3,19 (t, 2H, *J* = 6 Hz), 3.61 (m, 2H), 4.34 (t, 2H, *J* = 6 Hz), 6.74 (d, 1H, *J* = 9 Hz), 7.52 (dd, 1H, *J* = 7.5 and 8.5 Hz), 8.24 (d, 1H, *J* = 8.5 Hz), 8.39 (dd, 1H, *J* = 1 and 7.5 Hz), 8.49 (dd, 1H, *J* = 1 and 8.5 Hz). ^{13}C-NMR (CD_3OD, 125 MHz) δ: 22.7, 31.9, 32.3, 37.0, 44.6, 48.0, 52.6, 57.9, 105.5, 108.8, 121., 123.1, 125.4, 129.9, 131.6, 132.5, 136.3, 152.1, 165.7, 166.6, 172.6. HRMS (ESI) *m/z*: Calc. for $C_{24}H_{30}N_4O3$ ([M+H]$^+$): 423.2390, Found: 423.2396.

*4.1.10. Synthesis of 6-(azetidin-1-yl)-2-(2-(dimethylamino)-ethyl)-1*H*-benzo[*de*]isoquinoline-1,3(2*H*)-dione (**8a**)*

Azetidine (75 µL, 1.08 mmol) was added to a solution of the 6-bromo-naphthalimide **10a** [48] (65 mg, 0.18 mmol) in EtOH (5 mL) and the mixture was heated at 120ºC under MW irradiation for 1.5 h. Afterwards, the solvent was evaporated to dryness and the residue was purified by flash chromatography, using 1-10% gradient of MeOH in CH_2Cl_2 as eluent, to give the desired 6-(azetidin-1-yl)-naphthalimide **8a** as a yellow-orange solid (50 mg, 85 %). M.p. 152 ºC. HPLC-MS (5-95% gradient of A in B, 10 min) t_R = 5.25 min. ^{1}H-NMR (Cl_3CD, 400 MHz) δ: 2.31 (s, 6H), 2.50 (p, 2H, *J* = 7.5 Hz), 2.61 (t, 2H, J = 7 Hz), 4.25 (t, 2H, J = 7 Hz), 4.41 (t, 4H, *J* = 7.5 Hz), 6.30 (d, 1H, *J* = 8.5 Hz), 7.42 (dd, 1H, *J* = 7 and 8.5 Hz), 8.14 (dd, 1H, *J* = 1 and 8.5 Hz), 8.29 (d, 1H, *J* = 8.5 Hz), 8.45 (dd, 1H, *J* = 1 and 7 Hz). ^{13}C-NMR (CD_3Cl, 100 MHz) δ: 17.3, 38.0, 45.9, 55.6, 57.2, 106.5, 110.4, 121.2, 122.9, 123.9, 130.3, 130.9, 131.4, 133.6, 152.8, 164.3, 165.0. HRMS (ESI) *m/z*: Calc. for $C_{18}H_{20}N_4O_2$ ([M+H]$^+$): 324.1580, Found: 324.1586.

*4.1.11. Synthesis of 9-((*trans*-4-aminocyclohexyl)amino)-5-(2-(dimethylamino)ethyl)-4*H*-benzo[de][2,6]-naphthyridine-4,6(5*H*)-dione (**12b**)*

trans-1,4-Diaminocyclohexane (25.3 mg, 33.5 µL, 0.6 mmol) and DIPEA (6 µL, 0.05 mmol) were added to a solution of the 9-metoxi-quinolimide **2b** (45 mg, 0.40 mmol) in EtOH (5 mL) and the mixture was heated at 150ºC in a closed tube for 7 days. Afterwards, the solvent was evaporated to dryness and the residue was purified by flash chromatography, using 0-10 % MeOH in CH_2Cl_2 gradient as eluent, to give the desired quinolimide **12b** as red syrup (137 mg, 90%). HPLC-

MS (30-95% gradient of A in B, 10 min) t_R = 4.5 min. ^{1}H-NMR [CD_3OD, 400 MHz] δ: 1.44 (m, 4H)), 1.98 and 2.15 (2m, 4H), 2.25 (s, 6H), 2.54 (m, 2H), 2.87 (m, 1H), 3.58 (m, 1H), 4.15 (t, 2H, *J* = 7 Hz), 6.83 (d, 1H, *J* = 8.5 Hz), 8.12 (d, 1H, *J* = 4.5 Hz), 8.20 (d, 1H, *J* = 8.5 Hz), 8.83 (d, 1H, *J* = 4.5 Hz). ^{13}C-NMR (CD_3OD, 100 MHz) δ: 31.6, 33.1, 45.8, 50.7, 51.8, 57.8, 106.2, 107.9, 123.9, 125.3, 130.5, 135.9, 137.7, 148.4, 133.6, 150.9, 164.5, 165.0.

4.1.12. Synthesis of N-*(*trans*-4-((5-(2-(dimethylamino)ethyl)-4,6-dioxo-5,6-dihydro-4*H*-benzo[*de*][2,6]-naphthyridin-9-yl)amino)cyclohexyl)acetamide (**7b**)*

Ac_2O (1 ml) was added to a solution of the quinolimide **12b** (7 mg, 0.018 mmol) in dry CH_2Cl_2 (1 mL), and the mixture was stirred at room temperature for 1 h. Then, the solvent was removed under vacuum and the residue was purified by flash chromatography, using 0-5 % gradient of MeOH in CH_2Cl_2 as eluent to give the acetylated derivative **7b** as a red-orange solid (5 mg, 65 %). M.p. 230 ºC. HPLC-MS (30-95% gradient of A in B, 10 min) t_R = 5.65 min. ^{1}H-NMR (CD_3OD, 500 MHz) δ: 1.38 and 1.50 (2m, 4H), 1.84 (s, 3H) 1.94 and 2.12 (2m, 4H), 2.48 (s, 6H), 2.86 (t, 2H, *J* = 6.5 Hz), 3.60 (m, 2H), 4.26 (t, 2H, *J* = 6.5 Hz), 6.86 (d, 1H, *J* = 8.5 Hz), 8.17 (d, 1H, *J* = 4.5 Hz), 8.25 (d, 1H, *J* = 8.5 Hz), 8.87 (d, 1H, *J* = 4.5 Hz). ^{13}C- NMR (CD_3OD, 125 MHz) δ 22.7, 30.7, 32.1, 37.8, 45.3, 52.0, 57.8, 64.3, 106.2, 107.6, 124.1, 125.5, 130.5, 136.2, 137.9, 148.4, 151.3, 164.9, 165.4, 172.6. HRMS (ESI) *m/z*: Calc. for $C_{23}H_{29}N_5O_3$ ($[M+H]^+$): 424.2343, Found: 424.2340.

4.2. Photophysical methods

Excitation and emission spectra of compounds were determined for 12 μM solutions in solvents of diverse polarity. The spectra were recorded between 300 and 690 nm (0.5 nm increments and 0.1 s integration time) with excitation set at the appropriate excitation wavelength. Slit widths were set to 15 nm for excitation and to 6 or 20 nm for emission, depending on the observed emission intensity. All the spectra were corrected for background fluorescence by subtracting a blank scan of the solvent solution.

Fluorescence quantum yield determination. Fluorescence quantum yields (Φ_F) were determined in solvents of diverse polarity, and calculated with reference to a standard, which was selected depending on the photophysical properties of the corresponding fluorophore [49-51]. Coumarine 153 in EtOH (Φ = 0.53) was used as reference, except for **1a** and **2a,b** that were calculated with reference to quinine sulphate dihydrate in 0.1 M H_2SO_4 (Φ = 0.55). A 12 μM solution of the corresponding fluorophore was compared to a 12 μM solution of the standard to assure that the absorbance is less than 0.1 at identical excitation wavelengths. The following equation was used to calculate the quantum yield:

$$\Phi = \frac{I_x A_r n^2_x \Phi_r}{A_x I_r n^2_r}$$

where x and r denote the sample and standard, respectively, A is the absorption at the excitation wavelength, I is the integrated fluorescence intensity, and n is the refractive index of the solvent.

4.3. HTS Cytotoxicity assays in tumor cells

A colorimetric assay, using the sulforhodamine B (SRB) reaction, was adapted for a quantitative measurement of cell growth and viability, following the technique described by Skehan, P. A. *et al*. [52]. Cells (MDA-MB-231, A549, HT-29 and PSN1) were seeded in 96 well microtiter plates, at 5×10^3 cells per well in aliquots of 195 μL of RPMI medium, and they were allowed to attach to the plate surface by growing in drug free medium for 18 h. Afterwards, samples were added in aliquots of 5 μL [dissolved in (3:7) DMSO/H_2O]. After 48 h exposure, cells were fixed by adding 50 μL of cold 50% (w/v) trichloroacetic acid, and incubating at 4 ºC for 60 min. Then, the plates were washed with deionized H_2O and dried. 100 μL of SRB solution (0.4% w/v in 1% acetic acid) was added to each microtiter well and these were incubated at room temperature for 10 min. Unbound SRB was removed by washing with 1% acetic acid, the plates were air dried, and the bound stain was solubilized with Tris buffer. Optical densities were read on an automated spectrophotometer plate reader at a single wavelength of 490 nm. Data analysis was automatically generated by the high throughput screening LIMS implemented at the laboratory. The three response parameters GI_{50} (50% cell growth inhibition), LC_{50} (50% lethal concentration), and TGI (total growth inhibition) were extracted from concentration-response curves by linear interpolation, according to the National Cancer Institute (NCI) protocols [53].

4.4. Macrophage culture and fluorescence visualization

Macrophages RAW 264.7 (ECACC, Sigma P11) were used for testing our naphthalimide and quinolimide-based fluorophores as imaging probes. The cells were cultured in Dulbecco's modified Eagle's medium enriched with 100 mg/L of sodium piruvate supplemented with 10% fetal bovine serum (FBS), 200 mM L-glutamine, 100 u/mL penicillin and 100 μg/mL of streptomycin (complete medium). The cell culture was maintained in humidified atmosphere at 37 ºC, with 5 % of CO_2 and 95 % of air. The morphology of the cells was studied with an epifluorescence microscope Nikon TE-2000 and with the confocal Laser microscope (CLSM) Leica TCS SP2 with 7 lines of laser (457, 477, 488, 496, 514, 543, 633 nm).

RAW 264.7 cells were grown to a density of 8 x 10^4 cells/mL in complete medium, in 24-well plates incubated for 24 hours. After this time, half of the growing wells were treated with LPS (Polysaccharides of Escherichia coli, Sigma Aldrich, Spain) at a concentration of 5 μg/mL for 2 h and, then, treated with the fluorophores (5 μM). The other half of the wells was treated directly with the flourophores at the same concentration. The cells were left in the presence of the

fluorophores for 1 or 2 h. After this time, the cells were fixed with glutaraldehyde (2.5% v/v in H_2O) for 15 minutes. They were washed with distilled water twice and mounted and observed under the microscope. The images of cells treated with our products were compared with images obtained with the commercial nuclear fluorescent sensor DAPI (Invitrogen).

4.5. DNA Binding

The studies were carried out by means of titrations at a constant concentration of fluorophore (16 μM for **7a** and 20 μM for **7b**), using UV-visible spectrometry and circular dichroism (CD). The equipment used was the Jasco J-815 spectropolarimeter. Experimental conditions: 10 mM phosphate buffer, pH = 7.10, T = 25 ° C, (200 mM NaCl only in the titrations with the oligonucleotide). Inverse titrations, of a 4.3 μM concentration of the oligonucleotide R-13 with increasing concentrations of the fluorophores **7a** and **7b** (0-430 μM) were also carried out.

Conflict of interest

The authors have no conflicts of interest to declare.

Acknowledgements

The work was supported by grants SAF2012-32209, FU2015-67284-R, CTQ2017-85658-R form the Spanish Ministerio de Economía y Competividad, Agencia Estatal de Investigación and the European Regional Development Fund; and the CSIC grant 201580E073.

Supplementary Material

Supplementary material to this article can be found online at

References

[1] G.S. Loving, M. Sainlos, B. Imperiali, Monitoring protein interactions and dynamics with solvatochromic fluorophores, Trends Biotechnol., 28 (2010) 73-83.

[2] Z. Yang, J. Cao, Y. He, J.H. Yang, T. Kim, X. Peng, J.S. Kim, Macro-/micro-environment-sensitive chemosensing and biological imaging, Chem. Soc. Rev., 43 (2014) 4563-4601.

[3] A.S. Klymchenko, Y. Mely, Fluorescent environment-sensitive dyes as reporters of biomolecular interactions, Prog. Mol. Biol. Transl. Sci., 113 (2013) 35-58.

[4] A.S. Klymchenko, Solvatochromic and Fluorogenic Dyes as Environment-Sensitive Probes: Design and Biological Applications, Acc. Chem. Res., 50 (2017) 366-375.

[5] A. Kellmann, Intersystem crossing and internal conversion quantum yields of acridine in polar and nonpolar solvents, J. Phys. Chem., 81 (1977) 1195-1198.

[6] K. Kalyanasundaram, J.K. Thomas, Solvent-dependent fluorescence of pyrene-3-carboxaldehyde and its applications in the estimation of polarity at micelle-water interfaces, J. Phys. Chem., 81 (1977) 2176-2180.

[7] J.S. Seixas de Melo, R.S. Becker, A.L. Macanita, Photophysical behavior of coumarins as a function of substitution and solvent: Experimental evidence for the existence of a lowest lying 1(n,π*) state, J. Phys. Chem., 98 (1994) 6054-6058.

[8] S. Singha, D. Kim, B. Roy, S. Sambasivan, H. Moon, A.S. Rao, J.Y. Kim, T. Joo, J.W. Park, Y.M. Rhee, T. Wang, K.H. Kim, Y.H. Shin, J. Jung, K.H. Ahn, A structural remedy toward bright dipolar fluorophores in aqueous media, Chemical science, 6 (2015) 4335-4342.

[9] D. Singharoy, S. Chowdhury, S.S. Mati, S. Ghosh, K. Chattopadhyay, S.C. Bhattacharya, Photoinduced electron transfer switching mechanism of a naphthalimide derivative with its solvatochromic behaviour: An experimental and theoretical study with in cell investigations, Chem. - Eur. J., 23 (2017) 16516-16524.

[10] H. Zhu, J. Fan, H. Mu, T. Zhu, Z. Zhang, J. Du, X. Peng, d-PET-controlled "off-on" polarity-sensitive probes for reporting local hydrophilicity within lysosomes, Sci. Rep., 6 (2016) 35627.

[11] F. Fueyo-González, J.A. González-Vera, I. Alkorta, L. Infantes, M.L. Jimeno, M. Fernández-Gutiérrez, M.C. González-García, A. Orte, R. Herranz, Fluorescence mechanism switching from ICT to PET by substituent chemical manipulation: Macrophage cytoplasm imaging probes, Dyes and Pigments, 175 (2020) 108172.

[12] J.B. Grimm, B.P. English, J. Chen, J.P. Slaughter, Z. Zhang, A. Revyakin, R. Patel, J.J. Macklin, D. Normanno, R.H. Singer, T. Lionnet, L.D. Lavis, A general method to improve fluorophores for live-cell and single-molecule microscopy, Nat. Methods, 12 (2015) 244-250.

[13] A. Fernández, M. Vendrell, Smart fluorescent probes for imaging macrophage activity, Chem. Soc. Rev., 45 (2016) 1182-1196.

[14] Y. Li, T.-M. Liu, Discovering macrophage functions using In Vivo optical imaging techniques, Front. Immunol., 9 (2018) 502/501-502/520.

[15] J.S. Yoo, S.-C. Lee, Z.Y. Jow, P.Y.X. Koh, Y.-T. Chang, A Macrophage-Specific Fluorescent Probe for Intraoperative Lymph Node Staging, Cancer Res., 74 (2014) 44-55.

[16] K.A. Zachariasse, M. Grobys, T. von der Haar, A. Hebecker, Y.V. Il'ichev, Y.B. Jiang, O. Morawski, W. Kühnle, Intramolecular charge transfer in the excited state. Kinetics and configurational changes, J.Photochem. Photobiol., A, 102 (1996) 59-70.

[17] C.J. Joedicke, H.P. Luethi, Time-dependent density functional theory (TDDFT) study of the excited charge-transfer state formation of a series of aromatic donor-acceptor systems, J. Am. Chem. Soc., 125 (2003) 252-264.

[18] S. Banerjee, E.B. Veale, C.M. Phelan, S.A. Murphy, G.M. Tocci, L.J. Gillespie, D.O. Frimannsson, J.M. Kelly, T. Gunnlaugsson, Recent advances in the development of 1,8-naphthalimide based DNA targeting binders, anticancer and fluorescent cellular imaging agents, Chem. Soc. Rev., 42 (2013) 1601-1618.

[19] M.F. Braña, J.M. Castellano, C.M. Roldan, A. Santos, D. Vazquez, A. Jimenez, Synthesis and mode(s) of action of a new series of imide derivatives of 3-nitro-1,8-naphthalic acid, Cancer Chemother. Pharmacol., 4 (1980) 61-66.

[20] M.F. Braña, A.M. Sanz, J.M. Castellano, C.M. Roldan, C. Roldan, Synthesis and cytostatic activity of benz[de]isoquinoline-1,3-diones. Structure-activity relationships, Eur. J. Med. Chem., 16 (1981) 207-212.

[21] M. Chau, J.L. Christensen, A.M. Ajami, R.L. Capizzi, Amonafide, a topoisomerase II inhibitor, is unaffected by P-glycoprotein-mediated efflux, Leuk. Res., 32 (2008) 465-473.

[22] Y.H. Hsiang, J.B. Jiang, L.F. Liu, Topoisomerase II-mediated DNA cleavage by amonafide and its structural analogs, Mol. Pharmacol., 36 (1989) 371-376.

[23] M.F. Braña, A. Gradillas, Á. Gómez, N. Acero, F. Llinares, D. Muñoz-Mingarro, C. Abradelo, F. Rey-Stolle, M. Yuste, J. Campos, M.A. Gallo, A. Espinosa, Synthesis, biological activity, and quantitative structure-activity relationship study of azanaphthalimide and arylnaphthalimide derivatives, J. Med. Chem., 47 (2004) 2236-2242.

[24] P. Gao, W. Pan, N. Li, B. Tang, Fluorescent probes for organelle-targeted bioactive species imaging, Chem. Sci., 10 (2019) 6035-6071.

[25] H. Zhu, J. Fan, J. Du, X. Peng, Fluorescent Probes for Sensing and Imaging within Specific Cellular Organelles, Acc. Chem. Res., 49 (2016) 2115-2126.

[26] W. Ma, S. Zhang, Z. Tian, Z. Xu, Y. Zhang, X. Xia, X. Chen, Z. Liu, Potential anticancer agent for selective damage to mitochondria or lysosomes: Naphthalimide-modified fluorescent biomarker half-sandwich iridium (III) and ruthenium (II) complexes, Eur. J. Med. Chem., 181 (2019) 111599.

[27] H. Yu, Y. Xiao, L. Jin, A Lysosome-Targetable and Two-Photon Fluorescent Probe for Monitoring Endogenous and Exogenous Nitric Oxide in Living Cells, J. Am. Chem. Soc., 134 (2012) 17486-17489.

[28] L. He, Y. Li, C.-P. Tan, R.-R. Ye, M.-H. Chen, J.-J. Cao, L.-N. Ji, Z.-W. Mao, Cyclometalated iridium(iii) complexes as lysosome-targeted photodynamic anticancer and real-time tracking agents, Chem. Sci., 6 (2015) 5409-5418.

[29] W. Ma, L. Guo, Z. Tian, S. Zhang, X. He, J. Li, Y. Yang, Z. Liu, Rhodamine-modified fluorescent half-sandwich iridium and ruthenium complexes: potential application as bioimaging and anticancer agents, Dalton Trans., 48 (2019) 4788-4793.

[30] J. Li, Z. Tian, Z. Xu, S. Zhang, Y. Feng, L. Zhang, Z. Liu, Highly potent half-sandwich iridium and ruthenium complexes as lysosome-targeted imaging and anticancer agents, Dalton Trans., 47 (2018) 15772-15782.

[31] W. Ma, X. Ge, L. Guo, S. Zhang, J. Li, X. He, Z. Liu, Bichromophoric anticancer drug: Targeting lysosome with rhodamine modified cyclometalated Iridium(III) complexes, Dyes and Pigments, 162 (2019) 385-393.

[32] S. Uchiyama, K. Takehira, T. Yoshihara, S. Tobita, T. Ohwada, Environment-sensitive fluorophore emitting in protic environments, Org. Lett., 8 (2006) 5869-5872.

[33] M.M. Yusupov, G.Z. Yusupova, A. Baucom, K. Lieberman, T.N. Earnest, J.H.D. Cate, H.F. Noller, Crystal structure of the ribosome at 5.5 Å resolution, Science, 292 (2001) 883-896.

[34] R.M. Martin, H. Leonhardt, M.C. Cardoso, DNA labeling in living cells, Cytometry, Part A, 67A (2005) 45-52.

[35] R.W. Dirks, H.J. Tanke, Styryl molecules light-up RNAs, Chem. Biol., 13 (2006) 559-560.

[36] G. Song, Y. Sun, Y. Liu, X. Wang, M. Chen, F. Miao, W. Zhang, X. Yu, J. Jin, Low molecular weight fluorescent probes with good photostability for imaging RNA-rich nucleolus and RNA in cytoplasm in living cells, Biomaterials, 35 (2014) 2103-2112.

[37] N. Stevens, N. O'Connor, H. Vishwasrao, D. Samaroo, E.R. Kandel, D.L. Akins, C.M. Drain, N.J. Turro, Two color RNA intercalating probe for cell imaging applications, J. Am. Chem. Soc., 130 (2008) 7182-7183.

[38] N.A. O'Connor, N. Stevens, D. Samaroo, M.R. Solomon, A.A. Marti, J. Dyer, H. Vishwasrao, D.L. Akins, E.R. Kandel, N.J. Turro, A covalently linked phenanthridine-ruthenium(II) complex as a RNA probe, Chem. Commun. , (2009) 2640-2642.

[39] C.Y.Y. Yu, W. Zhang, R.T.K. Kwok, C.W.T. Leung, J.W.Y. Lam, B.Z. Tang, A photostable AIEgen for nucleolus and mitochondria imaging with organelle-specific emission, J. Mater. Chem. B, 4 (2016) 2614-2619.

[40] X. Ma, R. Sun, J. Cheng, J. Liu, F. Gou, H. Xiang, X. Zhou, Fluorescence aggregation-caused quenching versus aggregation-induced emission: A visual teaching technology for undergraduate chemistry students, J. Chem. Educ., 93 (2016) 345-350.

[41] A. Schreer, C. Tinson, J.P. Sherry, K. Schirmer, Application of Alamar blue/5-carboxyfluorescein diacetate acetoxymethyl ester as a noninvasive cell viability assay in primary hepatocytes from rainbow trout, Anal. Biochem., 344 (2005) 76-85.

[42] N.J. Buurma, I. Haq, Calorimetric and spectroscopic studies of Hoechst 33258: Self-association and binding to non-cognate DNA, J.Mol. Biol., 381 (2008) 607-621.

[43] L. Hahn, N.J. Buurma, L.H. Gade, A Water-soluble tetraazaperopyrene dye as strong G-quadruplex DNA binder, Chem. Eur. J., 22 (2016) 6314-6322.

[44] P. Thordarson, Determining association constants from titration experiments in supramolecular chemistry, Chem. Soc. Rev., 40 (2011) 1305-1323.

[45] J.B. Chaires, Analysis and interpretation of ligand-DNA binding isotherms, Methods in Enzymol., 340 (2001) 3-22.

[46] E.C. Long, J.K. Barton, On demonstrating DNA intercalation, Acc. Chem. Res., 23 (1990) 271-273.

[47] P.H. Grayshan, A.M. Kadhim, A.T. Peters, Heterocyclic derivatives of naphthalene-1,8-dicarboxylic anhydride. III. Benzo[k,l]thioxanthene-3,4-dicarboximides, J. Heterocycl. Chem., 11 (1974) 33-38.

[48] A. Pardo, E. Martin, J.M.L. Poyato, J.J. Camacho, J.M. Guerra, R. Weigand, M.F. Braña, J.M. Castellano, N-Substituted 1,8-naphthalimide derivatives as high efficiency laser dyes, J. Photochem. Photobiol., A, 48 (1989) 259-263.

[49] C. Würth, M. Grabolle, J. Pauli, M. Spieles, U. Resch-Genger, Relative and absolute determination of fluorescence quantum yields of transparent samples, Nat. Protoc., 8 (2013) 1535-1550.

[50] A.M. Brouwer, Standards for photoluminescence quantum yield measurements in solution (IUPAC technical report), Pure Appl. Chem., 83 (2011) 2213-2228.

[51] K. Rurack, M. Spieles, Fluorescence Quantum Yields of a Series of Red and Near-Infrared Dyes Emitting at 600-1000 nm, Anal. Chem., 83 (2011) 1232-1242.

[52] P. Skehan, R. Storeng, D. Scudiero, A. Monks, J. McMahon, D. Vistica, J.T. Warren, H. Bokesch, S. Kenney, M.R. Boyd, New colorimetric cytotoxicity assay for anticancer-drug screening, J. Natl. Cancer Inst., 82 (1990) 1107-1112.

[53] R.H. Shoemaker, The NCI60 human tumour cell line anticancer drug screen, Nat. Rev. Cancer, 6 (2006) 813-823.

Highlights

- New naphthalimide and quinolimide-based fluorophores are described
- Properties of naphthalimide-based fluorophores have been tuned by substituent manipulation
- DNA intercalating properties provide macrophage nucleus fluorescence imaging

Declaration of interests

☒ The authors declare that they have no known competing financial interests or personal relationships that could have appeared to influence the work reported in this paper.

☐The authors declare the following financial interests/personal relationships which may be considered as potential competing interests: